

Zeolite-Encapsulated Copper(II) Complexes of Pyridoxal-Based Tetradentate Ligands for the Oxidation of Styrene, Cyclohexene and Methyl Phenyl Sulfide

Mannar R. Maurya,^{*[a]} Baljit Singh,^[a] Pedro Adão,^[b] Fernando Avecilla,^[c] and João Costa Pessoa^[b]

Keywords: Zeolites / Copper(II) complexes / Heterogeneous catalysis / Oxidation reactions

Interaction of copper(II)-exchanged zeolite-Y with *N,N'*-ethylenebis(pyridoxyliminato) ($H_2pydx-en$, **I**) and *N,N'*-propylenebis(pyridoxyliminato) ($H_2pydx-1,3-pn$, **II**) ligands in refluxing methanol leads to the formation of the corresponding complexes, abbreviated herein as $[Cu(pydx-en)]-Y$ (**3**) and $[Cu(pydx-1,3-pn)]-Y$ (**4**), in the supercages of zeolite-Y. The neat complexes, $[Cu(pydx-en)]$ (**1**) and $[Cu(pydx-1,3-pn)]$ (**2**), have also been prepared with these ligands. Spectroscopic studies (IR, UV/Vis and EPR), elemental analyses, thermal studies, field emission scanning electron micrographs (FE-SEM) and X-ray diffraction patterns have been used to characterise these complexes. The crystal and molecular structures of **1** and of **2**·CH₃OH, have been determined, confirming the ONNO binding mode of the ligands. The geometry around the metal ion is very slightly distorted square-planar in **1** and distorted square-pyramidal in **2**. The encapsulated complexes catalyse the oxidation, by H₂O₂ and *tert*-butyl hydroperoxide, of styrene, cyclohexene and thioanisole efficiently. Under optimised reaction conditions, the oxidation of styrene catalysed by **3** and **4** gave 23.6% and 28.0% con-

version, respectively, using *tert*-butyl hydroperoxide as oxidant, where styrene oxide, benzaldehyde, benzoic acid and phenylacetaldehyde are the major products. Better conversions have been obtained using H₂O₂ as oxidant. Oxidation of cyclohexene catalysed by these complexes gave cyclohexene oxide, 2-cyclohexen-1-ol, cyclohexane-1,2-diol and 2-cyclohexen-1-one as the major products. A maximum of 90.1% conversion of cyclohexene with **3** and 83.0% with **4** was obtained under optimised conditions. Similarly, a maximum of 80.3% conversion of methyl phenyl sulfide with **3** and 81.0% with **4** was observed, where the selectivity of the major product methyl phenyl sulfoxide was found to be about 60%. Tests for the recyclability and heterogeneity of the reactions have also been carried out, and the results indicate their recyclability. A possible reaction mechanism has been proposed by titrating a methanol solution of **1** and **2** with H₂O₂ to identify the possible intermediates.

(© Wiley-VCH Verlag GmbH & Co. KGaA, 69451 Weinheim, Germany, 2007)

Introduction

Zeolites find applications in many scientific disciplines as catalysts and in all types of chemical engineering process technologies. The exchangeable property of extra-framework cations and suitable cavity size of the zeolites allow their modification by inclusion of chemically interesting molecules. A homogeneous catalyst, for example, a metal complex, may be considered one such interesting molecule and hence the term zeolite-encapsulated metal complexes. The large size of the encapsulated homogeneous catalysts and their rigidity make it difficult for them to escape the zeolite cages. Zeolite-encapsulated metal complexes having good catalytic activities possess the advantages of solid

heterogeneous catalysts and share many of the advantageous features of homogeneous catalysts.

The flexible nature of salen-type [$H_2salen = N,N'$ -bis(salicylidene)ethane-1,2-diamine] ligands has provided opportunities to design various transition-metal complexes in the nanocavity of zeolites and to develop catalytic processes for various reactions. Poltowicz et al. have encapsulated a whole range of metallosalen complexes {e.g., $[Fe(salen)]$, $[Mn(salen)]$, $[Cu(salen)]$ and $[Co(salen)]$ } in zeolite-X to study their catalytic activity for the oxidation of cyclooctane.^[1] Ratnasamy and co-workers have used copper(II) and manganese(III) complexes of salen derivatives encapsulated in the cavity of zeolite-X and zeolite-Y for the oxidation of styrene under aerobic conditions using *tert*-butyl hydroperoxide as an oxidant. The catalytic efficiency of these encapsulated complexes was much higher than that of the neat complexes. Electron-withdrawing substituents such as Cl, Br and NO₂ on the aromatic ring enhance the rate of oxidation.^[2,3] These complexes also catalyse the oxidation of phenol and *p*-xylene.^[4,5] Epoxidations of cyclohexene, cyclooctene, 1-hexene and other various types of alkenes, arenes and cycloalkenes, catalysed by different

[a] Department of Chemistry, Indian Institute of Technology Roorkee, Roorkee 247667, India

E-mail: rkmanfcy@iitr.ernet.in

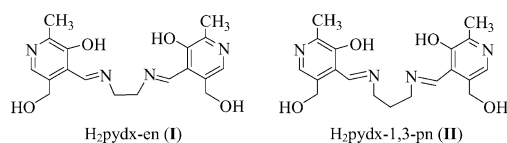
[b] Centro Química Estrutural, Instituto Superior Técnico – TU Lisbon,

Av. Rovisco Pais, 1049-001 Lisboa, Portugal

[c] Departamento de Química Fundamental, Facultad de Ciencias, Universidade da Coruña, Zapateira s/n, 15071 A Coruña, Spain

complexes of salen-type ligands, have also been carried out.^[6–9] [Co(salophen)]-Y [H_2 salophen = *N,N'*-bis(salicylidene)benzene-1,2-diamine] and related derivatives catalysed the oxidation of β -isophorone (β IP) to ketoisophorone (KIP) (along with other minor products) in the presence of an oxidant at ambient conditions of temperature and pressure.^[10] Liquid-phase oxidation of phenol with H_2O_2 has been reported using copper(II) and oxidovanadium(IV) complexes of *N,N'*-bis(salicylidene)propane-1,3-diamine (H_2 sal-1,3-pn) and *N,N'*-bis(salicylidene)diethylenetriamine (H_2 saldien).^[11–13] Copper(II) and oxidovanadium(IV) complexes of *N,N'*-bis(salicylidene)cyclohexane-1,2-diamine (H_2 sal-dach) catalyse the oxidation of styrene, cyclohexene and cyclohexane efficiently.^[14]

The catalytic potential of metal complexes encapsulated in the nanocavity of zeolites prompted us to design new zeolite-Y-encapsulated copper(II) complexes of tetradentate ligands **I** and **II** (Scheme 1). Catalytic potentials of these complexes have been demonstrated by studying the oxidation of styrene, cyclohexene and methyl phenyl sulfide. Copper(II), nickel(II) and oxidovanadium(IV) complexes of **I** have been reported previously.^[15,16] The structure of [Ni(pydx-en)] has been confirmed by single-crystal X-ray diffraction,^[17] while other complexes have been characterised by elemental analysis and spectroscopic techniques. We have also prepared neat copper(II) complexes of **I** and **II** to evaluate their catalytic potential and characterised them by single-crystal X-ray diffraction.

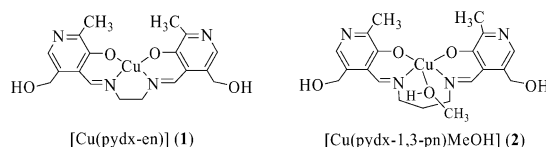


Scheme 1.

Results and Discussion

Synthesis and Characterisation of Catalysts

Scheme 2 presents the complexes prepared in this study. Their structures are based on elemental analysis and various spectroscopic studies, as well as on X-ray structure determinations. The presence of very strong peaks corresponding to $CuLH^+$ and $CuLNa^+$ in the ESI-MS spectra (positive mode) of DMSO solutions of **1** and **2**, with the correct isotope ratios, also confirms the integrity of the complexes in solution.



Scheme 2.

Reaction of cupric acetate with ligands H_2 pydx-en (**I**) and H_2 pydx-1,3-pn (**II**) in refluxing methanol yielded [Cu(pydx-en)] (**1**) and [Cu(pydx-1,3-pn)(MeOH)] (**2**), respectively. Complex **1** has previously been isolated by treating **I** with cupric acetate in aqueous solution.^[16] Encapsulation of these complexes in the nanocavities of zeolite-Y involved the exchange of copper(II) ion with Na-Y in water followed by reaction of the metal-exchanged zeolite-Y with **I** or **II** in methanol. This method is referred to as the flexible ligand method. Here, the ligands enter into the cavity of zeolite-Y because of their flexible nature and interact with the metal ion to give [Cu(pydx-en)]-Y (**3**) and [Cu(pydx-1,3-pn)]-Y (**4**). Finally, extraction of impure samples with methanol using a Soxhlet extractor removed excess free ligand, and stirring in DMF removed neat metal complex formed on the surface of the zeolite, if any. As the crude mass was well extracted, the metal content found after encapsulation is only due to the presence of copper(II) complexes in the supercages of the zeolite-Y. The diagonal dimension of the complexes is about 12 Å {in [Cu(pydx-en)]} or about 11 Å {in [Cu(pydx-1,3-pn)(MeOH)]}, which suggests that they will fit nicely into the supercages of zeolite-Y. The molecular formulae of the encapsulated complexes are based on the respective neat complex. The Si/Al ratio of 9.67 of zeolite-Y taken here corresponds to a unit cell formula $Na_{18}(AlO_2)_{18}(SiO_2)_{174}$. The estimated number of copper atoms per unit cell is 2.5 for [Cu(pydx-en)]-Y (**3**) and 2.4 for [Cu(pydx-1,3-pn)]-Y (**4**).

Structure Description of [Cu(pydx-en)] (**1**) and [Cu(pydx-1,3-pn)(MeOH)] (**2**)

Figures 1 and 2 include ORTEP representations of the molecular structure of [Cu(pydx-en)] (**1**) and [Cu(pydx-1,3-pn)(MeOH)] (**2**), respectively, and Table 1 provides selected bond lengths and angles of these compounds. The molecules are neutral, as both phenol groups are deprotonated, and the ligands coordinate to the Cu atom through two phenolate oxygen ($O_{phenolate}^-$) atoms and two imine nitrogen (N_{imine}) atoms. The geometry around the metal ion is slightly distorted square-planar in **1** and distorted square-pyramidal in **2**. A methanol molecule occupies the fifth coordination position in **2**.

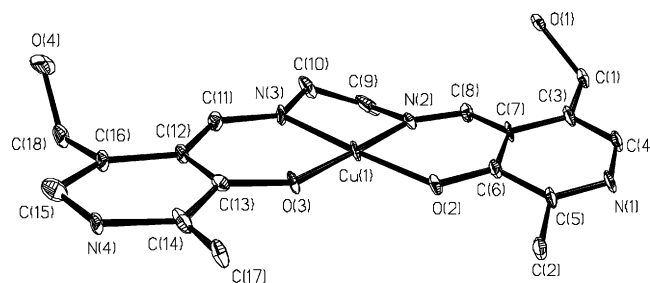


Figure 1. ORTEP diagram of [Cu(pydx-en)] (**1**) showing the atom labelling scheme. The thermal ellipsoids were drawn at the 30% probability level.

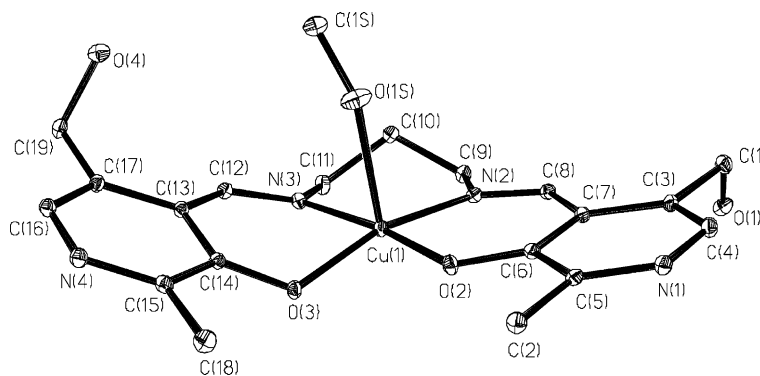


Figure 2. ORTEP diagram of [Cu(pydx-1,3-pn)(MeOH)] (**2**) showing the atom-labelling scheme. The thermal ellipsoids were drawn at the 30% probability level.

Table 1. Selected bond lengths [Å] and angles [°] for [Cu(pydx-en)] (**1**) and [Cu(pydx-1,3-pn)(MeOH)] (**2**).

Bond lengths [Å] for [Cu(pydx3-en)] (1)		Bond lengths [Å] for [Cu(pydx-1,3-pn)(MeOH)] (2)	
Cu(1)–O(2)	1.742(6)	Cu(1)–O(2)	1.8965(9)
Cu(1)–N(3)	1.796(7)	Cu(1)–O(3)	1.9546(9)
Cu(1)–O(3)	2.341(7)	Cu(1)–N(3)	1.9932(11)
Cu(1)–N(2)	2.373(9)	Cu(1)–N(2)	1.9935(11)
O(3)–C(13)	1.333(11)	Cu(1)–O(1S)	2.3525(11)
O(2)–C(6)	1.380(12)	O(2)–C(6)	1.2934(15)
N(2)–C(8)	1.256(12)	N(2)–C(8)	1.2962(16)
N(2)–C(9)	1.377(11)	N(2)–C(9)	1.4775(16)
N(3)–C(11)	1.434(13)	O(3)–C(14)	1.2998(15)
N(3)–C(10)	1.690(9)	N(3)–C(12)	1.2905(16)
C(6)–C(7)	1.609(15)	N(3)–C(11)	1.4670(16)
C(7)–C(8)	1.338(13)	C(6)–C(7)	1.4096(17)
C(11)–C(12)	1.695(15)	C(7)–C(8)	1.4443(17)
C(12)–C(13)	1.330(13)	C(9)–C(10)	1.5149(18)
		C(10)–C(11)	1.5198(19)
		C(12)–C(13)	1.4494(17)
		C(13)–C(14)	1.4082(17)
Angles [°] for [Cu(pydx-1,3-en)] (1)		Angles [°] for [Cu(pydx-1,3-pn)(MeOH)] (2)	
O(2)–Cu(1)–N(3)	175.2(3)	O(2)–Cu(1)–N(3)	169.92(4)
O(2)–Cu(1)–O(3)	90.0(3)	O(2)–Cu(1)–O(3)	82.08(4)
N(3)–Cu(1)–O(3)	94.8(3)	O(3)–Cu(1)–N(3)	87.94(4)
O(2)–Cu(1)–N(2)	91.2(3)	O(2)–Cu(1)–N(2)	92.29(4)
N(3)–Cu(1)–N(2)	84.1(3)	N(3)–Cu(1)–N(2)	97.76(4)
O(3)–Cu(1)–N(2)	178.8(2)	O(3)–Cu(1)–N(2)	166.61(4)
		O(2)–Cu(1)–O(1S)	90.18(4)
		O(3)–Cu(1)–O(1S)	94.46(5)
		N(3)–Cu(1)–O(1S)	89.23(4)
		N(2)–Cu(1)–O(1S)	97.71(5)
Lengths [Å] and angles [°] of hydrogen bonds in complexes			
O(1)⋯H(1), 0.82; O(1)⋯O(3), 2.563(8)		O(1)⋯H(1O), 0.69(2); O(1)⋯O(3), 2.7954(14)	
O(3)⋯H(1), 2.00; O(1)–H(1)–O(3), 125.5		O(3)⋯H(1O), 2.11(2); O(1)–H(1O)–O(3), 171(2)	
O(4)⋯H(4), 0.82; O(4)⋯N(1), 2.582(11)		O(1S)⋯H(1S), 0.64(3); O(1S)⋯N(1), 2.8037(16)	
N(1)⋯H(4), 2.01; O(4)–H(4)–N(1), 126.5		N(1)⋯H(1S), 2.16(3); O(1S)–H(1S)–N(1), 175(3)	
		O(4)⋯H(4O), 0.69(2); O(4)⋯N(4), 2.7959(15)	
		N(4)⋯H(4O), 2.12(2); O(4)–H(4O)–N(4), 166(2)	
Deviations from the planarity of the rings			
Ring: Cu(1)–O(2)–C(6)–C(7)–C(8)–N(2)		Ring: Cu(1)–O(2)–C(6)–C(7)–C(8)–N(2)	
Dev.: 0.0799(52) Å		Dev.: 0.0516(07) Å	
Ring: Cu(1)–N(2)–C(9)–C(10)–N(3)		Ring: Cu(1)–N(2)–C(9)–C(10)–C(11)–N(3)	
Dev.: 0.0976(48) Å		Dev.: 0.2239(08) Å	
Ring: Cu(1)–N(3)–C(11)–C(12)–C(13)–O(3)		Ring: Cu(1)–N(3)–C(12)–C(13)–C(14)–O(3)	
Dev.: 0.0334(50) Å		Dev.: 0.1928(07) Å	
Pyridoxal rings:		Pyridoxal rings:	
Planar, rms 0.0244(63) and 0.0172(60) Å		Planar, rms 0.0037(08) and 0.0083(09) Å	
Torsion angle between rings: 9.58 (0.57)°		Torsion angle between rings: 34.27(0.05)°	

The planar arrangement Cu(ONNO) is distorted, the *cis/trans* angles not being 90° and 180°. The *cis* angles are 90.0(3), 94.8(3), 91.2(3) and 84.1(3)° in **1**, and 82.08(4), 87.94(4), 92.29(4) and 97.76(4)° in **2**, and the *trans* angles are 175.2(3) and 178.8(2)° in **1**, and 169.92(4) and 166.61(4)° in **2**. The angles with the apical position of the O atom of the methanol molecule are 90.18(4), 94.46(5), 89.23(4) and 97.71(5)° in **2**.

In complex **1** the ligand forms a set of (6+5+6)-membered chelate rings, and the deviations from the planarity are listed in Table 1. The plane formed by the donor atoms N(2)–N(3)–O(2)–O(3) has a deviation from planarity of 0.0015(30) Å, and if the Cu^{II} ion is included, 0.0037(30) Å. In complex **2** the ligand forms a set of (6+6+6)-membered chelate rings, and the deviations from planarity are also listed in Table 1. The basal plane of the square pyramid formed by N(2)–N(3)–O(2)–O(3) atoms has a deviation from planarity of 0.1063(05) Å, and the Cu^{II} ion is 0.1020 Å above the plane. The Cu–O and Cu–N bond lengths (Table 1) are similar and in the usual range found for these compounds, 1.9–2.1 Å. The C–O distances are also typical for this type of ligands,^[15–21] and the C=N bonds are double bonds, with distances of about 1.3 Å.

In complex **1** the HO(CH₂) groups of the pyridoxal rings are in a *syn* position to each other, but in complex **2** the HO(CH₂) groups of the pyridoxal rings are in an *anti* conformation, similar to other complexes with this type of ligand.^[16] The pyridine nitrogen atoms and alcohol group of HO(CH₂) of the pyridoxal rings are involved in intermolecular H bonds. In complex **2**, the OH groups of the coordinated methanol molecule are also involved in H bonds. The bond lengths and angles of the hydrogen bonds are also included in Table 1.

Field Emission Scanning Electron Micrograph and Energy Dispersive X-ray Analysis Studies

Figure 3 presents the field emission scanning electron micrographs of [Cu(pydx-en)]-Y and [Cu(pydx-1,3-pn)]-Y. It is clear from the micrographs that zeolite-entrapped copper complexes have well-defined crystals, and there is no indication of the presence of any metal ions or complexes on the surface. Energy-dispersive X-ray analysis plots support this conclusion as no copper or nitrogen contents were noted on the spotted surface in plots for both catalysts. The average silicon and aluminium percentage obtained on the spotted surfaces were about 30% and 10%, respectively. An amount of about 3% sodium suggests the exchange of remaining free copper ions by sodium ions during the re-exchange process (see Experimental Section). Only a small amount of carbon (about 5%) but no nitrogen suggests the presence of a trace amount of solvent (methanol) from which it was finally washed after Soxhlet extraction. No morphological changes on the surface upon encapsulation of the complexes in the cavity are seen because of their poor loading.

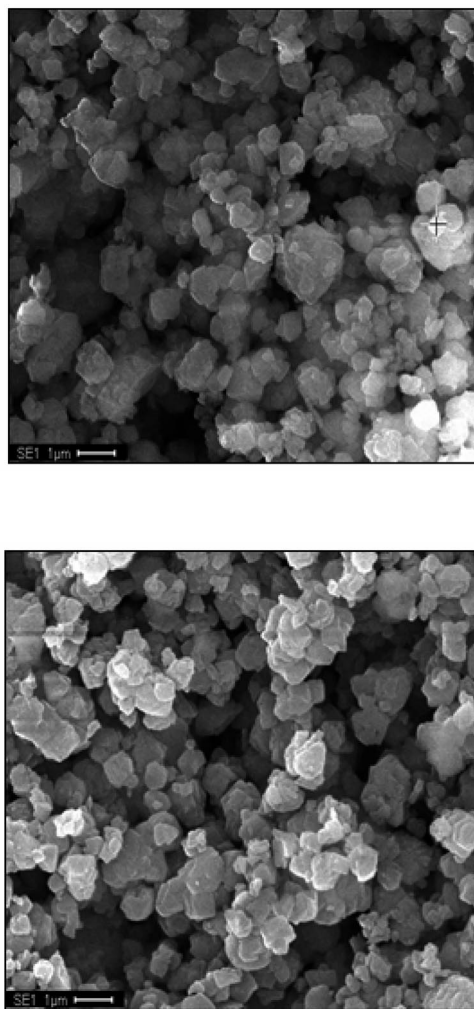


Figure 3. Field emission scanning electron micrograph of [Cu(pydx-en)]-Y (top) and [Cu(pydx-1,3-pn)]-Y (bottom).

Powder X-ray Diffraction Studies

The powder X-ray diffraction patterns of Na-Y, Cu-Y and encapsulated copper(II) complexes were recorded at 2θ values between 5 and 50°, and some representative patterns are presented in Figure 4. Essentially similar diffraction

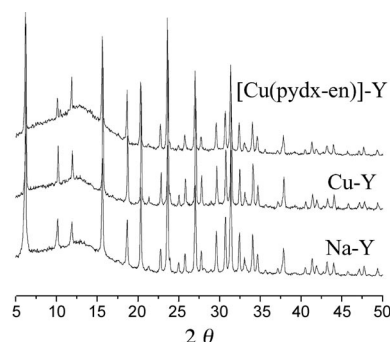


Figure 4. XRD patterns of Na-Y, Cu-Y and [Cu(pydx-en)]-Y (**3**).

patterns were noticed in encapsulated complexes Cu-Y and Na-Y, except zeolite with encapsulated metal complexes has a slightly weaker intensity. These observations indicate that the framework of the zeolites do not suffer any significant structural changes during encapsulation, that is, crystallinity of the zeolite-Y is preserved.

Thermogravimetric Analysis Studies

The decomposition of complexes **3** and **4** occurs in three overlapping steps. An endothermic loss of trapped water and methanol occurs between 80 and 200 °C, while exothermic removal of intra-zeolite water occurs between 300 and 350 °C. This is followed by endothermic loss of the ligand's residue, which continues until the removal of all organic mass at about 700 °C has occurred. The low percentage of weight loss (about 10%) for this last step indicates the presence of an only small amount of metal complexes in the cavities of the zeolite. This is in agreement with the low copper content estimated for these complexes. A weight loss of 6.9%, equivalent to methanol, in **2** occurs up to about 130 °C. The anhydrous complex is stable up to 260 °C, and then it decomposes in two major steps that are complete at 375 °C. The remaining residue of 18.1% slowly stabilises with the formation of a final residue of 17.5% (about 17.1% for CuO) at about 800 °C. A slightly different decomposition pattern has been obtained for **1**, where the decomposition of the stable complex starts at about 290 °C and occurs in two overlapping steps. The decomposition is complete at about 360 °C. The remaining residue of 20.6% further loses weight up to about 800 °C and stabilises at 18.3%. The calculated residue for CuO of 18.9% agrees with the value observed.

IR Spectral Studies

A partial list of IR spectroscopic data is presented in Table 2. The intensity of the peaks in encapsulated complexes is, however, weak because of their low concentration in zeolite matrix; the spectra of the encapsulated as well as neat complexes showed essentially similar bands. Comparison of the spectra of these complexes with the respective ligand provides evidence for the coordinating mode of ligands in complexes. The ligand H₂pydx-en exhibits a medium-intensity band around 2700 cm⁻¹ due to intramolecular hydrogen bonding. Absence of this band in the spectra of encapsulated complexes indicates the destruction of the

hydrogen bond followed by the coordination of the phenol oxygen atom after deprotonation. Existence of this band, however, in neat complexes hints towards the presence of hydrogen bonding. A sharp band appearing at 1626 cm⁻¹ (in **I**) or at 1632 cm⁻¹ (in **II**) due to the ν(C=N) (azomethine) shifts to higher wavenumbers in complexes, thereby suggesting the coordination of the azomethine nitrogen atom. Several multiple bands of medium intensity covering the region 2850–3000 cm⁻¹ are observed due to C–H bands. The spectral patterns of these complexes are similar to [Cu(pydx-en)] reported in the literature.^[16]

UV/Vis Spectral Studies

UV/Vis spectral studies of **I** and its copper(II) complex **1** have been discussed in detail in the literature.^[16] Other complexes reported here exhibit very similar spectral patterns. The well-defined band at 590 nm in **1** and a broad band covering the region 570–650 nm in **2** have been assigned to a d–d transition. Such a d–d band in zeolite-encapsulated complexes could not be obtained because of their poor loading, while ligand bands appearing in the UV region are similar to those observed for neat complexes. This data is collected in Table 2 and the spectra of encapsulated complexes are presented in Figure 5.

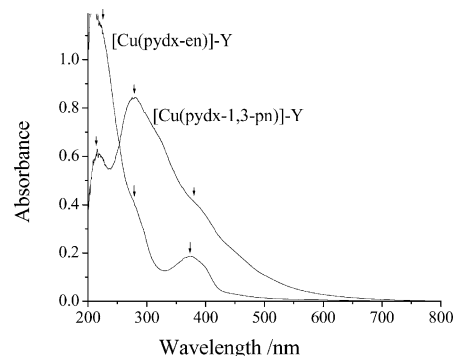


Figure 5. UV/Vis spectra of [Cu(pydx-en)]-Y and [Cu(pydx-1,3-pn)]-Y dispersed in nujol.

EPR Studies

The EPR spectra of the neat Cu^{II} complexes **1** and **2** in the polycrystalline state are broad because of dipolar and spin–spin exchange interactions. It is clear that they are characterised by an axial **g** tensor, but the hyperfine features

Table 2. IR and UV/Vis spectroscopic data of ligand, pure and encapsulated complexes.

Compound	IR [cm ⁻¹]		Solvent	UV/Vis
	ν(OH)	ν(C=N)		λ _{max} [nm]
H ₂ pydx-en (I)	3280–3450	1626	CH ₃ OH	216, 252, 335
H ₂ pydx-1,3-pn (II)	2846–3480	1632	CH ₃ OH	215, 252, 334
[Cu(pydx-en)] (1)	ca. 3400	1634	CH ₃ OH	235, 277, 378
[Cu(pydx-1,3-pn)(MeOH)] (2)	ca. 3450	1635	CH ₃ OH	233, 273, 377
[Cu(pydx-en)]-Y (3)	ca. 3400	1633	nujol	207, 283, 374
[Cu(pydx-1,3-pn)]-Y (4)	ca. 3450	1638	nujol	217, 246, 402

were not resolved, neither at room temperature nor at 77 K, and not much structural information can be obtained. The EPR spectra of the neat Cu^{II} complexes **1** and **2** in DMF solutions, and of the catalysts **3** and **4** are given in Figures 6 and 7.

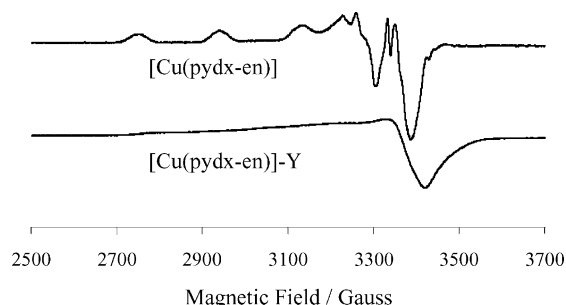


Figure 6. EPR spectra of a frozen DMF solution of $[\text{Cu}(\text{pydx-en})]$ (**1**) and of $[\text{Cu}(\text{pydx-en})]\text{-Y}$ (**3**) at room temperature.

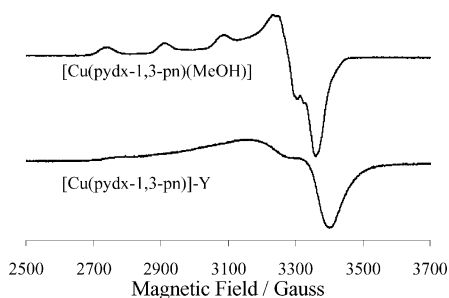


Figure 7. EPR spectra of a frozen DMF solution of $[\text{Cu}(\text{pydx-1,3-pn})(\text{MeOH})]$ (**2**) and of $[\text{Cu}(\text{pydx-1,3-pn})]\text{-Y}$ (**4**) at room temperature.

The spectra of the encapsulated complexes **3** and **4** are reasonably resolved, indicating the encapsulation of individual molecules in the supercages of Na-Y. The intermolecular interactions are avoided because of isolation of the zeolite cavities, indicating that the Cu^{II} sites are well separated in the catalyst, and thereby the spin Hamiltonian parameters can be estimated with reasonable accuracy; these are listed in Table 3.

Both neat complexes **1** and **2** have an N_2O_2 binding mode and are monomeric in the solid state. Complex **1** has a square-planar configuration, and **2** has square-planar configuration with a pyramidal distortion. In DMF solutions the representation of the A_{\parallel} , g_{\parallel} values fit well with those of other $[\text{Cu}^{\text{II}}(\text{salen})]$ complexes.^[5,22–25] The $g_{\parallel}/A_{\parallel}$ ratio is 112.7 for **1**, indicating a remarkable planarity of the square-planar geometry, as found in the solid state. For **2** this ratio is 126, but this is mainly due to a decrease in A_{\parallel} . Very sim-

ilar g_{\parallel} and A_{\parallel} parameters and $g_{\parallel}/A_{\parallel}$ ratios were found for $[\text{Cu}^{\text{II}}(\text{salen})]$ (2.212 , $203.7 \times 10^{-4} \text{ cm}^{-1}$, 109 , respectively) and $[\text{Cu}^{\text{II}}(\text{sal-1,3-pn})]$ (2.254 , $172.5 \times 10^{-4} \text{ cm}^{-1}$, 131 , respectively),^[25] in DMF solutions, indicating very similar geometries and balance of charge to those of **1** and **2**. No super-hyperfine structure is distinguished.

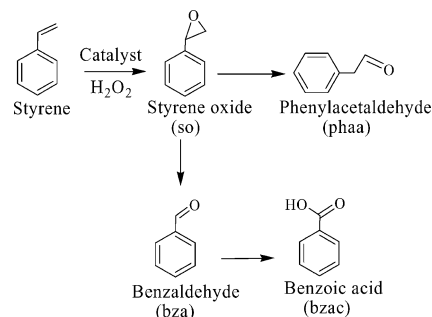
The EPR spectra of the encapsulated complexes were recorded at room temperature and are broader than those for frozen solutions, suggesting that the complexes located in the supercages may be present in more than one geometrical conformation. However, the g_{\parallel} and A_{\parallel} parameters and $g_{\parallel}/A_{\parallel}$ ratios ($g_{\parallel}/A_{\parallel} = 113$ for **3** and 126 for **4**) almost coincide with those obtained in DMF solutions, indicating similar geometries and balance of charge for the complexes in the encapsulated and dissolved forms.

Catalytic Activity Studies

The catalytic activities of the zeolite-encapsulated and neat complexes have been demonstrated by studying the oxidation of styrene, cyclohexene and methyl phenyl sulfide.

Oxidation of Styrene

The oxidation of styrene, catalysed by $[\text{Cu}(\text{pydx-en})]\text{-Y}$ and $[\text{Cu}(\text{pydx-1,3-pn})]\text{-Y}$, was carried out using H_2O_2 and *tert*-butyl hydroperoxide as oxidants to give styrene oxide, benzaldehyde, benzoic acid and phenylacetaldehyde (Scheme 3) along with minor amounts of unidentified products. Hulea and Dumitriu^[26] have reported some of these products while using catalysts TS-1 and MCM-41. All oxidation products as observed here were identified recently using the polymer-anchored catalyst PS- $[\text{VO}(\text{sal-ohyba})\text{-(DMF)}]$ ($\text{H}_2\text{sal-ohyba} = \text{Schiff base derived from salicylaldehyde and } o\text{-hydroxybenzylamine}$)^[27] and the zeolite-Y-encapsulated complex $[\text{VO}(\text{sal-dach})]\text{-Y}$.^[14]



Scheme 3.

Table 3. EPR data for $[\text{Cu}(\text{pydx-en})]$ and $[\text{Cu}(\text{pydx-1,3-pn})(\text{MeOH})]$ complexes as neat and encapsulated in zeolite-Y.

Complex	g_{xx}	g_{yy}	$g_{zz(\parallel)}$	A_{xx} ($\times 10^4 \text{ cm}^{-1}$)	A_{yy} ($\times 10^4 \text{ cm}^{-1}$)	$A_{zz(\parallel)}$ ($\times 10^4 \text{ cm}^{-1}$)
$[\text{Cu}(\text{pydx-en})]$ (1)	2.07	2.03	2.22	17.39	28.43	196.94
$[\text{Cu}(\text{pydx-1,3-pn})(\text{MeOH})]$ (2)	2.04	2.06	2.24	21.85	16.88	178.53
$[\text{Cu}(\text{pydx-en})]\text{-Y}$ (3)		2.08	2.32	–	–	156
$[\text{Cu}(\text{pydx-1,3-pn})]\text{-Y}$ (4)		2.09	2.34	–	–	138

In order to achieve the maximum oxidation of styrene, catalyst **3** was taken as a representative, and the effect of four different reaction parameters – viz. the amount of H_2O_2 (mol of H_2O_2 per mol of styrene), amount of catalyst, volume of solvent and temperature of the reaction – was studied.

Three different aqueous 30% H_2O_2 /styrene molar ratios of 1:1, 2:1 and 3:1 were considered while keeping the fixed amount of styrene (1.04 g, 10 mmol) and catalyst (0.025 g) in CH_3CN (20 mL) at 80 °C. The periodic analyses of results up to 6 h are illustrated in Figure 8. Increasing the H_2O_2 /styrene ratio from 1:1 to 2:1 improved the conversion from 9.1% to 14.8% while a 3:1 ratio showed a further increment of conversion of hardly 1%. Therefore, it is clear that the 2:1 molar ratio is quite suitable to obtain the optimum styrene conversion of 14.8% in the 6 h reaction time.

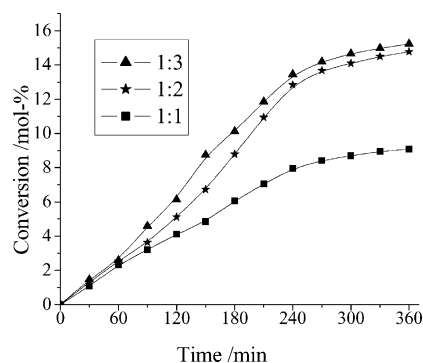


Figure 8. Effect of H_2O_2 on the oxidation of styrene. Reaction conditions: styrene (1.04 g, 10 mmol), $[\text{Cu}(\text{pydx-en})\text{-Y}]$ (**3**) (0.025 g), CH_3CN (20 mL) and temp. (80 °C).

Similarly, for three different amounts – viz. 0.015, 0.025 and 0.035 g – of $[\text{Cu}(\text{pydx-en})\text{-Y}]$ at a styrene/aqueous 30% H_2O_2 ratio of 1:2 under the above reaction conditions, 0.015 g of catalyst, achieved only 7.8% conversion, whereas 0.025 g of catalyst gave a maximum conversion of 14.8% in 6 h of reaction time. A further increment of catalyst (0.035 g) has shown no improvement (Figure 9). The reason for reduced activity at higher catalyst dose may be adsorption/chemisorption of the two reactants on separate catalyst particles, thereby reducing the chance to interact.

Figure 10 illustrates the oxidation of styrene at three different temperatures – viz. 60, 70 and 80 °C –, while keeping the optimised conditions of 10 mmol of styrene, 20 mmol of H_2O_2 and 0.025 g of catalyst in 20 mL of acetonitrile. It is evident from the figure that the performance of the catalyst is poor at 60 °C wherein only 3.9% conversion was observed. Increasing the reaction temperatures to 70 and 80 °C increases the conversion to 7.0% and 14.8%, respectively. Thus, conducting the catalytic reaction at 80 °C is most suitable to maximise the oxidation of styrene. We have also observed that reducing the volume of CH_3CN to 10 mL under the above optimised reaction conditions improved the conversion considerably, and two more components, though in poor yield, have also been obtained.

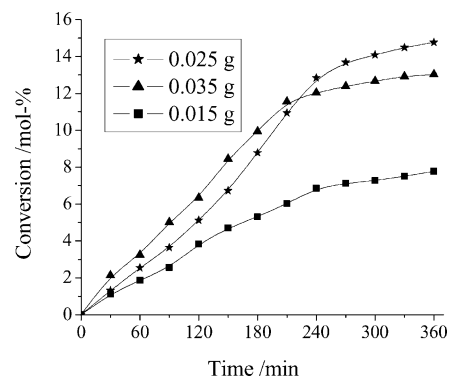


Figure 9. Effect of the amount of catalyst on the oxidation of styrene. Reaction conditions: styrene (1.04 g, 10 mmol), 30% H_2O_2 (2.27 g, 20 mmol), CH_3CN (20 mL) and temp. (80 °C).

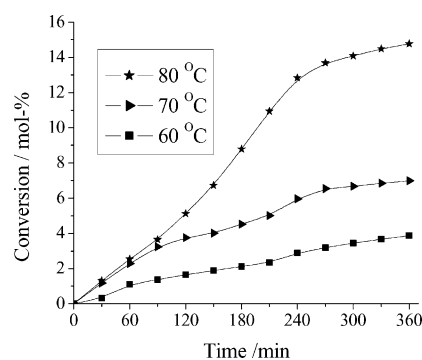


Figure 10. Effect of the temperature on the oxidation of styrene. Reaction conditions: styrene (1.04 g, 10 mmol), $[\text{Cu}(\text{pydx-en})\text{-Y}]$ (0.025 g), 30% H_2O_2 (2.27 g, 20 mmol) and CH_3CN (20 mL).

Thus, for the maximum oxidation of 10 mmol of styrene, the other required conditions as concluded were: $[\text{Cu}(\text{pydx-en})\text{-Y}]$ (0.025 g), H_2O_2 (2.27 g, 20 mmol), CH_3CN (10 mL) and temperature (80 °C). Under these optimised reaction conditions, the catalytic activities of **1–4** were further tested, and the results obtained are shown in Figure 11. Table 4 compares the selectivity of the various products obtained after 6 h of reaction time, along with the percent conversion of styrene and turnover frequency. It is clear from Table 4 and Figure 11 that $[\text{Cu}(\text{pydx-1,3-pn})\text{-Y}]$ exhibits 37.4% conversion, which is better than that exhibited by $[\text{Cu}(\text{pydx-en})\text{-Y}]$ (33.3%). Both catalysts gave mainly four products: styrene oxide, benzaldehyde, phenylacetaldehyde and benzoic acid. The selectivity for benzaldehyde is much higher, while the other products are obtained in small amounts.

We have also tested the catalytic activity of the neat complexes **1** and **2** for the oxidation of styrene using an equimolar concentration of metal ion as in their respective zeolite-encapsulated metal complex. Figure 11 also provides the conversion as a function of time, while Table 4 lists all other details. Thus, under the above reaction conditions, the conversion obtained by the neat complexes (18.7% for **1** and 22.3% for **2**) is significantly lower than that shown by the respective encapsulated complexes. Again, all four products have been obtained with the selectivity order: benzaldehyde > styrene oxide > phenylacetaldehyde > benzoic acid.

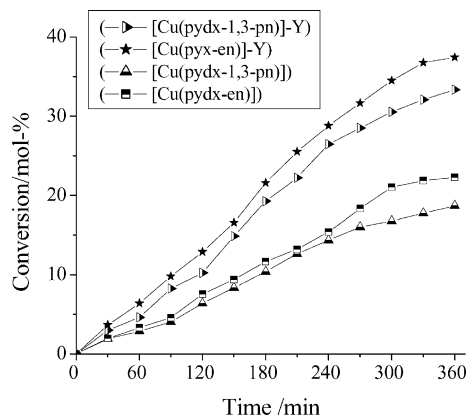


Figure 11. Catalytic comparison of zeolite-encapsulated and neat complexes for the oxidation of styrene in the presence of H_2O_2 as oxidant. Reaction conditions: styrene (1.04 g, 10 mmol), catalyst (0.025 g for encapsulated and 0.00133 g in the case of neat complexes), H_2O_2 (2.27 g, 20 mmol), CH_3CN (10 mL) and temp. (80°C).

Table 4. Product selectivity and percent conversion of styrene after 6 h of reaction time with H_2O_2 as oxidant.

Catalyst (H_2O_2)	Conv. (%)	Product selectivity (%)					TOF ^[a] [h^{-1}]
						Others	
[Cu(pydx-en)]-Y (3)	33.3	82.2	12.4	1.6	1.4	2.4	179
[Cu(pydx-1,3-pn)]-Y (4)	37.4	75.4	15.0	4.0	3.0	2.6	215
[Cu(pydx-en)] (1)	18.7	81.6	7.4	4.8	2.6	3.6	106
[Cu(pydx-1,3-pn)(MeOH)] (2)	22.3	79.4	9.9	6.2	3.0	1.5	128

[a] TOF [h^{-1}] (turnover frequency): mol of substrate converted per mol of metal (in the solid catalyst) per hour.

Under the above optimised reaction conditions, the catalytic action of neat as well encapsulated complexes has also been tested using *tert*-butyl hydroperoxide (TBHP) as an oxidant: 70% TBHP (2.57 g, 20 mmol), catalyst (0.025 g for encapsulated and 0.00133 g, for neat complexes) and styrene (1.04 g, 10 mmol) were used in CH_3CN (20 mL), and the reaction was carried out at 80°C . Figure 12 shows the conversion as a function of time, and Table 5 compares the selectivity data along with the conversion and turnover frequency after 6 h of reaction time. It is clear that the obtained percentage conversion varies in the range 13.6–28.0% with the order: [Cu(pydx-1,3-pn)]-Y (28.0%) > [Cu(pydx-en)]-Y (23.6%) > [Cu(pydx-1,3-pn)] (16.2%) > [Cu(pydx-en)] (13.6%). Thus, the overall conversion of styrene with TBHP is always lower than with H_2O_2 . The selectivity of the formation of an important component – styrene oxide – is better (43.4–70.5%), but two more products, namely benzoic acid and phenylacetaldehyde, have also been obtained.

The highest yield of benzaldehyde using H_2O_2 as oxidant is possibly due to further oxidation of styrene oxide formed in the first step by a nucleophilic attack of H_2O_2 on styrene oxide followed by cleavage of the intermediate hydroperoxystyrene.^[28] The formation of benzaldehyde may also be facilitated by the direct oxidative cleavage of the styrene side-chain double bond by a radical mechanism.^[27] Forma-

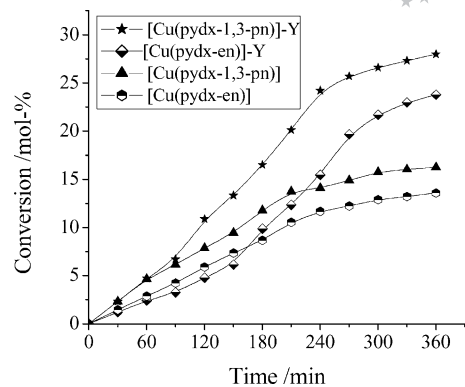


Figure 12. Catalytic comparison of zeolite-encapsulated metal complexes and neat complexes for the oxidation of styrene in the presence of TBHP as oxidant. Reaction conditions: styrene (1.04 g, 10 mmol), catalyst (0.025 g for encapsulated and 0.00133 g in case of neat complexes), TBHP (2.57 g, 20 mmol), CH_3CN (20 mL) and temp. (80°C).

Table 5. Product selectivity and percent conversion of styrene with TBHP after 6 h of reaction time.

Catalyst (TBHP)	Conv. (%)	Product selectivity (%)					TOF [h^{-1}]
						Others	
[Cu(pydx-en)]-Y (3)	23.6	60.7	30.8	0.8	1.3	6.4	127
[Cu(pydx-1,3-pn)]-Y (4)	28.0	43.4	33.1	0.8	2.4	20.3	160
[Cu(pydx-en)] (1)	13.6	70.5	21.0	0.6	1.8	6.1	77
[Cu(pydx-1,3-pn)(MeOH)] (2)	16.2	45.4	16.1	0.7	16.8	21.0	93

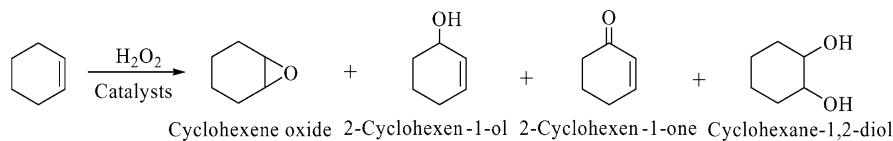
tion of other products such as phenylacetaldehyde is possible through isomerisation of styrene oxide, while the formation of benzoic acid from benzaldehyde is straightforward.

Oxidation of Cyclohexene

The oxidation of cyclohexene catalysed by encapsulated complexes gave cyclohexene oxide, 2-cyclohexen-1-ol, cyclohexane-1,2-diol and 2-cyclohexen-1-one, as shown in Scheme 4. Recently, we observed all these products while using catalyst [VO(sal-dach)] encapsulated in zeolite-Y.^[14]

The reaction conditions have been optimised considering **3** as a representative catalyst and varying the amount of catalyst, oxidant, solvent and temperature of the reaction mixture. The effect of H_2O_2 concentration on the oxidation of cyclohexene is shown in Figure 13. Three different H_2O_2 /cyclohexene molar ratios of 1:1, 2:1 and 3:1 were used at a fixed amount of cyclohexene (0.82 g, 10 mmol), catalyst (0.025 g), acetonitrile (20 mL) and temperature (75°C). From Figure 13 it is clear that a 3:1 molar ratio is the best of those tested, to obtain a conversion of 38.8% in 6 h.

The amount of catalyst has shown considerable affect on the oxidation of cyclohexene. For a cyclohexene/ H_2O_2 ratio of 1:3, five different amounts of catalyst – viz. 0.015, 0.025, 0.035, 0.050 and 0.065 g – were used under the above reaction conditions, and the results obtained are summarised in Figure 14. The conversion increases with an increase in the amount of catalyst from 0.015 to 0.050 g (28 to 56.2%), and



Scheme 4.

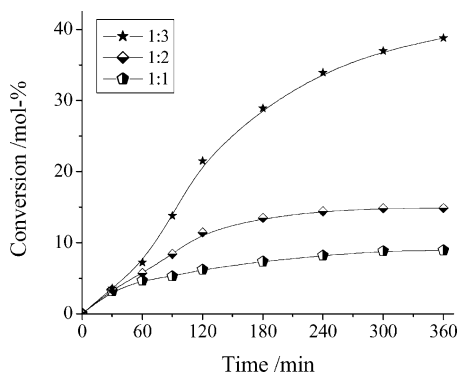


Figure 13. Effect of H_2O_2 on the oxidation of cyclohexene. Reaction conditions: cyclohexene (0.82 g, 10 mmol), $[\text{Cu}(\text{pydx-en})]\text{-Y}$ (0.025 g), CH_3CN (20 mL) and temp. (75°C).

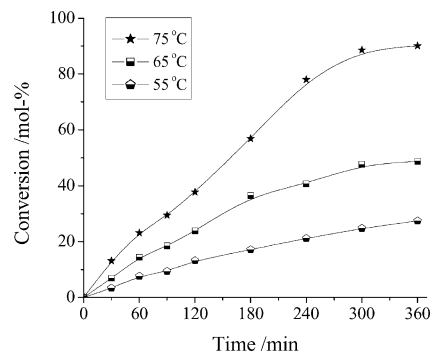


Figure 15. Effect of the temperature on the oxidation of cyclohexene. Reaction conditions: cyclohexene (0.82 g, 10 mmol), $[\text{Cu}(\text{pydx-en})]\text{-Y}$ (**3**) (0.050 g), 30% H_2O_2 (3.40 g, 30 mmol) and CH_3CN (10 mL).

then assumes a lower trend with 0.065 g of catalyst (52.4%). Thus, an amount of 0.050 g of catalyst is considered adequate to carry out the oxidation of cyclohexene. It was also noted that by reducing the volume of acetonitrile to 10 mL, this conversion reached 90.1% with 0.050 g of catalyst under the above reaction conditions.

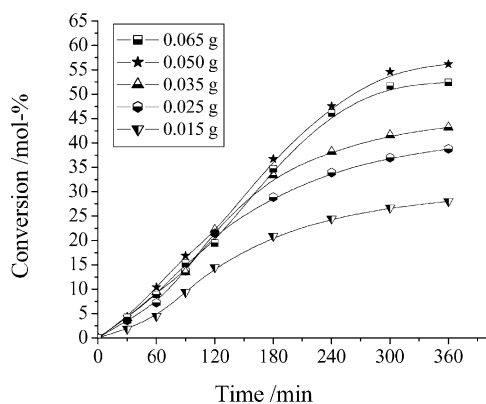


Figure 14. Effect of the amount catalyst on the oxidation of cyclohexene. Reaction conditions: cyclohexene (0.82 g, 10 mmol), 30% H_2O_2 (3.40 g, 30 mmol), CH_3CN (20 mL) and temp. (75°C).

Figure 15 illustrates the effect of temperature of the reaction medium on the conversion of cyclohexene as a function of time. Amongst the three different temperatures (55, 65 and 75°C) for the fixed amount of cyclohexene (0.82 g, 10 mmol), aqueous 30% H_2O_2 (3.40 g, 30 mmol) and catalyst (0.050 g) in acetonitrile (10 mL), running the reaction at 75°C has shown the best result, where 90.1% conversion has been obtained.

Thus, suitable reaction conditions for the maximum oxidation of cyclohexene were optimised as follows: cyclohexene (0.82 g, 10 mmol), H_2O_2 (3.40 g, 30 mmol), catalyst (0.050 g), acetonitrile (10 mL) and a temperature of 75°C . Catalyst **4** was also tested under the above reaction conditions, and results along with the selectivity of various reaction products are summarised in Table 6. A maximum of 83.0% conversion has been achieved with **4**, which is less than that obtained by **3** (90.1%) in 6 h of contact time. However, both catalysts show the highest selectivity towards the formation of 2-cyclohexen-1-ol, which is followed by cyclohexene oxide. The selectivity of the two other products, 2-cyclohexen-1-one and cyclohexane-1,2-diol, has no definite trend.

We have also tested the catalytic activities of encapsulated complexes using *tert*-butyl hydroperoxide as an oxidant. Thus, catalyst (0.050 g), *tert*-butyl hydroperoxide (3.855 g, 30 mmol) and cyclohexene (0.82 g, 10 mmol) were used in acetonitrile (10 mL), and the reaction was carried out at 75°C . The data, also presented in Table 6, show a poor conversion of cyclohexene (19.5% for **3** and 17.8% for **4**) with *tert*-butyl hydroperoxide in 6 h of contact time. Here, the major product obtained is cyclohexane-1,2-diol, while amounts of the other three products are very poor.

The neat complexes gave 45.5% (with 0.0028 g of **1**) or 50.7% (with 0.0027 g of **2**) conversion using H_2O_2 as an oxidant (Table 6). Here, the selectivity of cyclohexene oxide is better (33 to 38.7%) in comparison with the encapsulated complexes, although the overall selectivity orders of all products are the same. However, the turnover rates for encapsulated complexes, their stability towards decomposition and easy recovery from the reaction mixture make encapsulated complexes better catalysts than neat ones.

Table 6. Oxidation of cyclohexene and product selectivity using various catalysts.

Catalyst	Oxidant	Conv. (%)					Other	TOF [h ⁻¹]
[Cu(pydx-en)]-Y (3)	H ₂ O ₂	90.1	26.9	37.8	22.2	9.5	3.6	241
[Cu(pydx-1,3-pn)]-Y (4)	TBHP	19.5	1.4	2.4	2.5	92.9	0.8	52
	H ₂ O ₂	83.0	37.1	51.1	3.5	8.3	0.0	237
[Cu(pydx-en)] (1)	TBHP	17.8	1.5	2.0	3.1	92.5	0.9	51
	H ₂ O ₂	50.7	38.7	44.5	4.9	5.4	6.5	136
[Cu(pydx-1,3-pn)(MeOH)] (2)	H ₂ O ₂	45.5	33.0	51.5	5.0	4.9	5.6	130

The conversion of cyclohexene and selectivity of different reaction products using [Cu(pydx-1,3-pn)]-Y as catalyst under the optimised reaction conditions have been analysed as a function of time and are presented in Figure 16. It is clear from the plot that a selectivity of 20.7% of cyclohexene oxide and 35.5% of cyclohexen-1-ol has been obtained at a conversion of 20.2% of cyclohexene in 1 h of reaction time. The selectivity for these products increases with time and reaches 37.1% and 51.1%, respectively, with the increase of the conversion of cyclohexene to 83.0% in 6 h. The other two products, 2-cyclohexen-1-one and cyclohexane-1,2-diol, have 26.8% and 14.7% selectivity in the first hour, but their selectivities decrease with time and reach 3.5 and 8.2%, respectively. Thus, to obtain a good selectivity for the important product cyclohexene oxide, it is essential to run the reaction for at least 6 h under the optimised reaction conditions. After 6 h, only minor changes have been noted in the selectivities of the different reaction products.

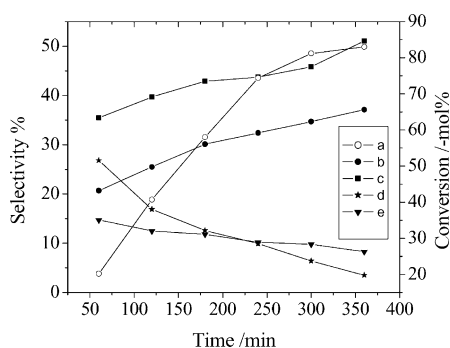
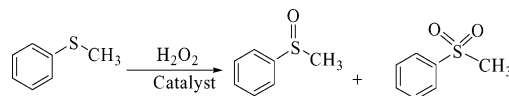


Figure 16. Conversion of cyclohexene and variation in the selectivity of various products as a function of time: (a) conversion of cyclohexene, (b) cyclohexene oxide, (c) 2-cyclohexen-1-ol, (d) 2-cyclohexen-1-one and (e) cyclohexane-1,2-diol.

Oxidation of Methyl Phenyl Sulfide (Thioanisol)

Enzyme sulfoxidases^[29] facilitate sulfide peroxidase activity where the electron-rich sulfur atom of the sulfide undergoes electrophilic oxidation by H₂O₂ to give the sulfoxide and, further, sulfone. Such oxidation of methyl phenyl sulfide was tested with the copper complexes prepared in this work. Oxidation of methyl phenyl sulfide in the presence of H₂O₂ gave two products, namely methyl phenyl sulfoxide and methyl phenyl sulfone, as shown in Scheme 5.



Scheme 5.

The catalytic potential of these catalysts has also been optimised considering the amount of oxidant, solvent and catalyst. Thus, catalyst 4 was taken as a representative, and the amount of oxidant was varied at a fixed amount of methyl phenyl sulfide (1.242 g, 10 mmol) and catalyst (0.025 g) in acetonitrile (10 mL), and the reaction was carried out at ambient temperature. At an aqueous H₂O₂/substrate ratio of 2:1, a maximum of 69.3% conversion was achieved in 3 h of reaction time. Decreasing this ratio to 1:1 decreases the conversion of methyl phenyl sulfide considerably, while increasing this ratio to 3:1 has a marginal effect on the conversion (Figure 17). The only significant influence when using a 3:1 ratio is the completion of the reaction in less time. Increasing the volume of solvent to 20 mL under the above reaction conditions decreases the conversion considerably (to 64.3%).

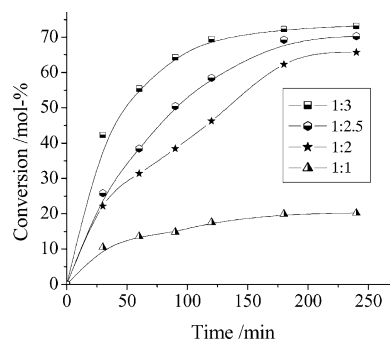


Figure 17. Effect of the amount of H₂O₂ on the oxidation of methyl phenyl sulfide as a function of time. Reaction conditions: methyl phenyl sulfide (1.242 g, 10 mmol), [Cu(pydx-1,3-pn)]-Y (0.025 g) and acetonitrile (10 mL).

Similarly, four different amounts of catalyst – viz. 0.015, 0.025, 0.035 and 0.050 g – were considered, while keeping methyl phenyl sulfide (1.242 g, 10 mmol) and 30% H₂O₂ (2.27 g, 20 mmol) in acetonitrile (10 mL). As mentioned in Figure 18, increasing the catalyst amount from 0.015 to 0.025 g increases the conversion from 46.8 to 69.3%. Increasing it to 0.035 g improves the conversion to 81.0%, while 0.050 g shows no improvement. Therefore, it is clear

that 0.035 g of catalyst is adequate to obtain an optimum methyl phenyl sulfide conversion of 81.0% in 3 h of contact time.

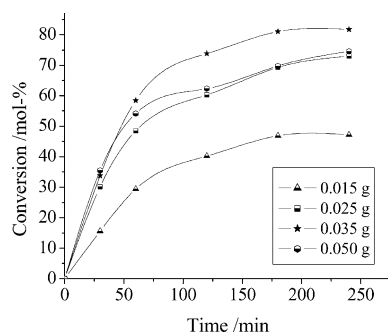


Figure 18. Effect of the amount of catalyst on the oxidation of methyl phenyl sulfide. Reaction conditions: methyl phenyl sulfide (1.242 g, 10 mmol), H_2O_2 (2.27 g, 20 mmol) and acetonitrile (10 mL).

Thus, under the optimised reaction conditions, that is, catalyst (0.035 g), methyl phenyl sulfide (1.242 g, 10 mmol), 30% H_2O_2 (2.27, 20 mmol) and acetonitrile (10 mL), catalyst **3** was also tested, and the results of both catalysts are compared in Figure 19, while Table 7 provides selectivity details. Under the optimised reaction conditions, **3** and **4** gave 80.3% and 81.0% conversion, respectively. In terms of the product selectivity, the selectivities of methyl phenyl sulfoxide and methyl phenyl sulfone are 63.3 and 36.7%, respectively, for **3** and 53.6 and 46.4%, respectively, for **4**. A blank reaction under similar conditions, that is, methyl phenyl sulfide (1.242 g, 10 mmol), aqueous 30% H_2O_2 (2.27 g, 20 mmol) and acetonitrile (10 mL), resulted in 35.2% conversion with 68.3% selectivity towards sulfoxide and 31.7% sulfone. Thus, catalysts **3** and **4** only enhanced the percent conversion of methyl phenyl sulfide and played no positive role in enhancing the selectivity of sulfoxide. In contrast, a positive role in enhancing the selectivity towards the formation of sulfoxide as well as conversion of methyl phenyl sulfide has been observed by oxidovanadium(IV) and copper(II) complexes encapsulated in the cavities of zeolite-Y.^[30] The neat complexes also exhibited a good catalytic activity (68.4–69.9% conversion) when 0.0019 g amounts were used under the above optimised conditions. However, the selectivity for sulfone was better than for sulfoxide.

Catalytic activities of these complexes have also been tested using TBHP as an oxidant under similar conditions. Again, 0.035 g of catalyst has shown the best results at a fixed amount of methyl phenyl sulfide (10 mmol) and TBHP (20 mmol) in acetonitrile (10 mL). A maximum of 47.1% conversion has been obtained with **3**, while **4** gave only 18.1% conversion in 3 h of reaction time (Figure 20). Neat complexes **1** and **2** exhibited very poor conversion of 4.7 and 4.2%, respectively. Independently of the catalytic systems and conversions, the sulfoxide has been obtained selectively with TBHP.

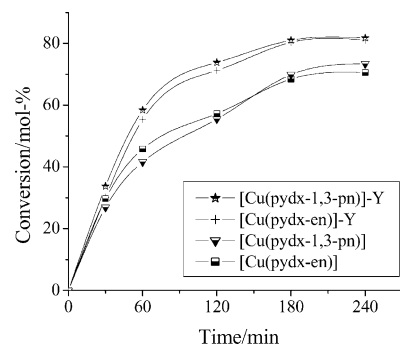
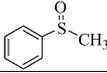
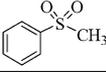


Figure 19. Oxidation of methyl phenyl sulfide by various catalysts using H_2O_2 as an oxidant.

Table 7. Conversion percentage of methyl phenyl sulfide in 3 h using H_2O_2 as an oxidant and selectivity of sulfoxide and sulfone.

Catalyst	Conv. (%)	Product selectivity (%)		TOF [h^{-1}]
				
[Cu(pydx-en)]-Y (3)	80.3	63.34	36.66	622
[Cu(pydx-1,3-pn)]-Y (4)	81.0	53.59	46.41	662
[Cu(pydx-en)] (1)	68.4	39.87	60.13	530
[Cu(pydx-1,3-pn)](MeOH) (2)	69.9	44.94	55.06	603

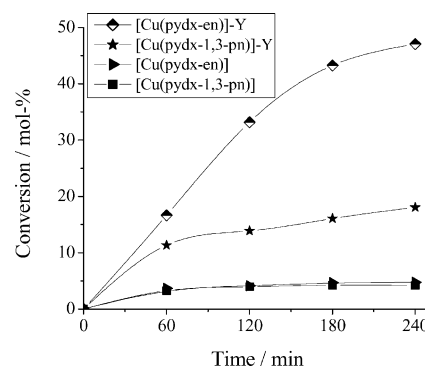


Figure 20. Oxidation of methyl phenyl sulfide by various catalysts using *tert*-butyl hydroperoxide as an oxidant.

Test for Recyclability and Heterogeneity of the Reactions

The recyclability of both the encapsulated complexes has been tested in all three catalytic reactions. In a typical experiment, for example, for styrene, after a contact time of 6 h, the reaction mixture was filtered, and after activating the catalyst by washing with acetonitrile and drying at 120 °C, it was subjected to a further catalytic reaction under similar conditions. No appreciable loss in catalytic activity suggests that the complex is still present in the cavity of zeolite-Y. The filtrate collected after separating the used catalyst was placed in the reaction flask and the reaction was continued after adding fresh oxidant for another 4 h. The gas chromatographic analysis showed no improvement in conversion, and this confirms that the reaction did not proceed upon removal of the solid catalyst. The reaction was, therefore, heterogeneous in nature.

Possible Reaction Pathway of the Catalysts

In order to better understand the reaction mechanism, the neat complexes were treated with H_2O_2 and the progress of the reaction was monitored by electronic absorption spectroscopy. Thus, titration of a solution of **1** (about 10^{-4} M) in methanol with one-drop portions of 30% H_2O_2 dissolved in methanol resulted in the spectral changes shown in Figure 21. The intensity of the band at 378 nm changes marginally, but the band at 277 nm increases considerably, while the band at 235 nm (not shown) continuously gains intensity. With a more concentrated solution (about 10^{-3} M) now dissolving complex **1** in DMSO, upon equivalent H_2O_2 additions the band appearing at 590 nm broadens with an increase in the intensity (Figure 21, inset). A very similar spectral pattern has also been observed for **2** (Figure 22). The data suggest the interaction of copper(II) complexes with H_2O_2 .

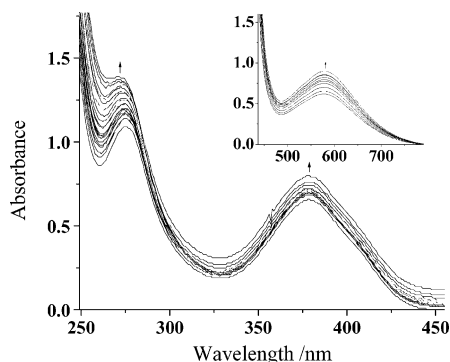


Figure 21. Titration of a methanol solution (about 10^{-4} M) of [Cu(pydx-en)] (**1**) with aqueous 30% H_2O_2 dissolved in methanol. The inset displays equivalent titrations, but with higher concentrations of **1** (about 10^{-3} M) dissolved in DMSO.

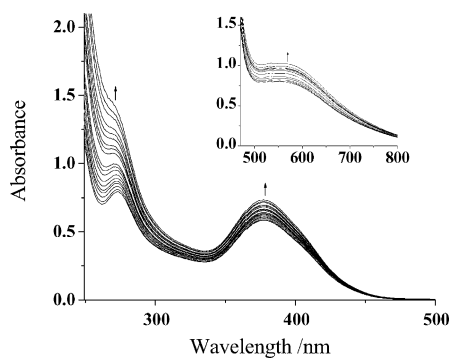


Figure 22. Titration of a methanol solution (about 10^{-4} M) of [Cu(pydx-1,3-pn)MeOH] (**2**) with aqueous 30% H_2O_2 dissolved in methanol. The inset displays equivalent titrations, but with higher concentrations of **2** (about 10^{-3} M) dissolved in DMSO.

At least three types of intermediates having a copper–oxygen interaction – side-on $\text{Cu}^{\text{III}}-(\mu-\eta^2\text{-peroxido})-\text{Cu}^{\text{III}}$, bis(μ -oxido- Cu^{III}) and $\text{Cu}^{\text{III}}-\text{O}-\text{O}-\text{H}$ (copper hydroperoxide) – have been discussed in the literature during the catalytic action.^[31,32] As copper complexes [Cu(pydx-en)] and

[Cu(pydx-1,3-pn)] are monomeric in the cavity of zeolite, the facile formation of intermediates [(HOO)-Cu(pydx-en)] and [(HOO)-Cu(pydx-1,3-pn)], respectively, are expected because of the vacant available site in them (for example complex **3** was characterised in the solid state with a coordinated methanol molecule). This intermediate is expected to transfer the oxygen atoms to the substrates to obtain the products. Thus, the catalytic performance of the supported catalyst could be attributed to the facile formation of this Cu hydroperoxide intermediate species. The broadening of the band at about 590 nm indicates the merging of the d–d band with this charge-transfer band because of Cu hydroperoxide complex formation. In fact characteristic charge-transfer bands because of Cu hydroperoxide coordination are known to appear around 590 nm.^[33]

Attempts to detect Cu hydroperoxide intermediates by ESI-MS (in the positive and negative modes) failed. The addition of H_2O_2 only increased the intensities of the peaks corresponding to CuLH^+ and CuLNa^+ (and $\text{CuL}\cdot 2\text{H}^{2+}$ for larger amounts of H_2O_2) in the positive mode, but no peaks could be found in the negative mode that we could assign to Cu hydroperoxide intermediate species.

Conclusions

Zeolite-Y-encapsulated copper(II) complexes [Cu(pydx-en)]-Y and [Cu(pydx-1,3-pn)]-Y with *N,N'*-ethylenebis(pyridoxyliminato) ($\text{H}_2\text{pydx-en}$) and *N,N'*-propylenebis(pyridoxyliminato) ($\text{H}_2\text{pydx-1,3-pn}$) ligands have been prepared. Neat complexes, [Cu(pydx-en)] and [Cu(pydx-1,3-pn)(MeOH)], have also been prepared with these ligands and characterised, and their crystal and molecular structures were determined, confirming the ONNO binding mode of the ligands. The encapsulated complexes catalyse the oxidation of styrene, cyclohexene and thioanisole efficiently, either using H_2O_2 or *tert*-butyl hydroperoxide as oxidants. Oxidation of styrene catalysed by [Cu(pydx-en)]-Y and [Cu(pydx-1,3-pn)]-Y gave 23.6% and 28.0% conversion, respectively, using TBHP as an oxidant. Using H_2O_2 as oxidant the major products were styrene oxide and benzaldehyde, while TBHP gave styrene oxide, benzaldehyde, benzoic acid and phenylacetaldehyde. Under the optimised conditions the maximum conversions obtained were 90.1% of cyclohexene, using [Cu(pydx-en)]-Y, and 83.0% using [Cu(pydx-1,3-pn)]-Y as catalyst; the major products identified were cyclohexene oxide, 2-cyclohexen-1-ol, cyclohexane-1,2-diol and 2-cyclohexen-1-one. Similarly, maximums of 80.3% conversion of methyl phenyl sulfide with [Cu(pydx-en)]-Y and of 81.0% with [Cu(pydx-1,3-pn)]-Y were observed, where the selectivity for the major product methyl phenyl sulfoxide was found to be about 60%. Tests for recyclability and heterogeneity of the reactions indicated their good recyclability. Of the alternative suggested mechanisms for catalysis, namely regarding the intermediates specifying the copper–oxygen interaction, our data suggest the involvement of $\text{Cu}^{\text{III}}-\text{O}-\text{O}-\text{H}$ (copper hydroperoxide) intermediates.

Experimental Section

Materials: Analytical reagent-grade pyridoxal hydrochloride (Hpydx·HCl, Himedia, Mumbai, India), methyl phenyl sulfide (Alfa Aeser, USA), styrene, cyclohexene (Acros Organics, NJ, USA), cupric nitrate (E. Merck, Mumbai, India) and 30% aqueous H₂O₂ (Qualigens, Mumbai, India) were used as obtained. Y-zeolite (Si/Al = 10) was obtained from Indian Oil Corporation (R&D), Faridabad, India. All other chemicals and solvents used were of AR grade. Ligands H₂pydx-en (**I**) and H₂pydx-1,2-pn (**II**) were prepared as described in the literature.^[15]

Physical Methods and Analysis: The copper content was measured using an inductively coupled plasma spectrometer (ICP; Labtam 8440 Plasmalab) after leaching the metal ions with conc. nitric acid and diluting with double-distilled water to specific volumes. IR spectra were recorded as KBr pellets with a Nicolet NEXUS Aligent 1100 series FTIR spectrophotometer, after grinding the sample with KBr. UV/Vis spectra of zeolite-encapsulated metal complexes were recorded in Nujol using a Shimadzu 1601 UV/Vis spectrophotometer by layering a mull sample to the inside of one of the cuvettes and keeping the other one layered with Nujol as reference. UV/Vis spectra of other ligands and neat complexes were recorded in methanol. X-ray powder diffractograms of solid catalysts were recorded using a Bruker AXS D8 advance X-ray powder diffractometer with a Cu-K_α target. Thermogravimetric analyses of pure as well as encapsulated complexes were carried out using a TG Stanton Redcroft STA 780 instrument. Scanning electron micrographs (SEM) of zeolite-containing samples were recorded with a Leo instrument, model 435VP. The samples were dusted on alumina and coated with a thin film of gold to prevent surface changing and to protect the surface material from thermal damage by the electron beam. In all analyses, a uniform thickness of about 0.1 mm was maintained. The energy-dispersive X-ray analysis (EDAX) plots of encapsulated complexes were recorded with an FEI Quanta 200 FEG instrument. The ESI-MS data were obtained with a Varian 500-MS LC ion-trap mass spectrometer operating either in the positive or in the negative mode. The EPR spectra were recorded with a Bruker ESP 300E X-band spectrometer. The spectra were measured at room temperature and at 77 K (with glasses, made by freezing solutions in liquid nitrogen, or just using the frozen samples). For the neat complexes we recorded spectra in DMF and in DMSO. In DMSO apparently there was precipitation of solids upon freezing, as only broad signals were obtained. The spin Hamiltonian parameters were obtained by simulation of the spectra with the computer program of Rockenbauer and Korecz.^[34] All catalysed reaction products were analysed using a Thermoelectron gas chromatograph fitted with an HP-1 capillary column (30 m × 0.25 mm × 0.25 μm) and FID detector. Styrene, cyclohexene and methyl phenyl sulfide were used as external standards to quantify their conversion upon catalytic action. To quantify the conversion of styrene, for example, the calibration of the GC was carried out using styrene as external standard by injecting three different but known concentrations of styrene into the GC under the reaction conditions at which the analyses of catalytic products were performed and noting the peak area in each case. Finally, the peak area obtained for the remaining amount of styrene during catalytic oxidation was correlated with the peak area of the standard sample. This ultimately gave the percent conversion of substrate. The selectivity of products was then obtained directly from the peak areas of the respective products. Other external standards were used similarly. The identities of the products were confirmed by GC-MS with a Perkin-Elmer Clarus 500 model.

X-ray Crystal Structure Determination: Three-dimensional X-ray data were collected with a Bruker Kappa Apex CCD diffractometer by the ϕ - ω scan method. Data were collected at room temperature. Reflections were measured from a hemisphere of data collected from frames each covering 0.3° in ω . Of the 13687 reflections measured for **1** and 20715 for **2**, all of which were corrected for Lorentz and polarization effects, and for absorption by semiempirical methods based on symmetry-equivalent and repeated reflections, 2139 independent reflections for **1** and 8116 for **2** exceeded the significance level $|F|/\sigma(|F|) > 4.0$. Complex scattering factors were taken from the program package SHELXTL.^[35] The structures were solved by direct methods and refined by full-matrix least-squares methods on F^2 . The hydrogen atoms were included in calculated positions and refined by using a riding mode for **1** and were left to refine freely for **2**. Refinement converged with allowance for thermal anisotropy of all non-hydrogen atoms. Minimum and maximum final electron density: 2.494 and -2.167 e Å⁻³ for **1**, 0.997 and -0.673 e Å⁻³ for **2**. Crystal data and details on data collection and refinement are summarised in Table 8. CCDC-655305 (for **1**) and -655304 (for **2**) contain the supplementary crystallographic data for this paper. These data can be obtained free of charge from the Cambridge Crystallographic Data Centre via www.ccdc.cam.ac.uk/data_request/cif.

Table 8. Crystal data collection and refinement.

	1	2
Empirical formula	C ₁₈ H ₂₀ CuN ₄ O ₄	C ₂₀ H ₂₆ CuN ₄ O ₅
M_r [g mol ⁻¹]	419.92	465.99
Crystal system	triclinic	triclinic
Space group	$P\bar{1}$	$P\bar{1}$
T [K]	293(2)	293(2)
a [Å]	9.6664(17)	8.0870(2)
b [Å]	10.0904(19)	9.0492(2)
c [Å]	10.150(3)	14.2599(3)
α [°]	101.418(14)	105.8640(10)
β [°]	93.432(14)	90.9030(10)
γ [°]	116.898(9)	95.5120(10)
V [Å ³]	852.7(4)	998.20(4)
$F(000)$	434	486
Z	2	2
$D_{\text{calcd.}}$ [g cm ⁻³]	1.636	1.550
μ [mm ⁻¹]	1.315	1.135
R_{int}	0.0918	0.0334
Measured reflections	13687	20715
Observed reflections	2139	8116
Data/restraints/parameters	2975/3/248	10700/0/375
Goodness-of-fit on F^2	1.093	1.029
R_1 ^[a]	0.0918	0.0415
wR_2 ^[b] (all data)	0.2713	0.1029

[a] $R_1 = \sum ||F_o| - |F_c|| / \sum |F_o|$. [b] $wR_2 = \{ \sum [w(|F_o|^2 - |F_c|^2)]^2 / \sum [w(F_o^4)] \}^{1/2}$.

Preparations

Preparation of [Cu(pydx-en)] (1**):** A stirred solution of H₂pydx-en (0.717 g, 2 mmol) dissolved in methanol (20 mL) was added to cupric acetate (0.40 g, 2 mmol) dissolved in methanol (30 mL) with stirring, and the reaction mixture was refluxed in a water bath for 5 h. On reducing the solvent volume to about 20 mL and keeping the mixture at ambient temperature, a brown solid of [Cu(pydx-en)] slowly separated within a few hours. This was filtered off, washed with methanol and dried in vacuo over silica gel. Yield: 78%. Green crystals suitable for X-ray diffraction study were ob-

tained from the filtrate on slow concentration at room temperature. $C_{18}H_{20}CuN_4O_4$ [Cu(pydx-en)] (419.93): calcd. C 51.48, H 4.80, Cu 15.13, N 13.34; found C 52.0, H 4.6, Cu 15.1, N 13.1.

Preparation of [Cu(pydx-1,3-pn)(MeOH)] (2): [Cu(pydx-1,3-pn)(MeOH)] was prepared according to essentially the same procedure as for **1**. A green solid was obtained. Green crystals suitable for X-ray diffraction study were obtained from the filtrate on keeping it at room temperature for slow concentration. Yield: 70%. $C_{20}H_{26}CuN_4O_5$ [Cu(pydx-1,3-pn)(MeOH)] (466.0): calcd. C 51.55, H 5.62, Cu 13.64, N 12.02; found C 51.8, H 5.8, Cu 13.8, N 12.2.

Preparation of Cu-Y: Na-Y zeolite (5.0 g) was suspended in distilled water (300 mL) and after addition of cupric nitrate (2.26 g, 12 mmol), the reaction mixture was heated at 90 °C with stirring for 24 h. The pale bluish solid was filtered, washed with hot distilled water until the filtrate was free from any copper(II) ion content and dried at 150 °C in an air oven for 24 h. Found: Cu 7.60.

Preparation of [Cu(pydx-en)]-Y (3): Cu-Y (3.0 g) and $H_2pydx-en$ (3.0 g) were mixed in methanol (50 mL), and the reaction mixture was heated under reflux in an oil bath with stirring for 14 h. The resulting material was filtered and then Soxhlet-extracted with methanol to remove unreacted ligand. It was finally treated with hot DMF while stirring for 1 h, filtered and washed with DMF followed by hot methanol. The uncomplexed metal ions present in the zeolite were removed by stirring with double-distilled aqueous NaCl (0.01 M, 150 mL) for 10 h. The resulting pale yellow solid was filtered, and washed with hot distilled water until no precipitate of AgCl was observed in the filtrate on treating with $AgNO_3$. Finally it was dried at 120 °C for several hours. Found: Cu 0.79.

Preparation of [Cu(pydx-1,3-pn)]-Y (4): The pale yellow [Cu(pydx-1,3-pn)]-Y was prepared according to essentially the same procedure as outlined for **3**. Found: Cu 0.74.

Catalytic Activity

Oxidation of Styrene: The catalytic oxidation of styrene was carried out in 50-mL flasks fitted with a water-circulated condenser. In a typical reaction, an aqueous solution of 30% H_2O_2 or 70% *tert*-butyl hydroperoxide (TBHP) (20 mmol) and styrene (1.04 g, 10 mmol) was mixed in acetonitrile (20 mL). After the temperature of the oil bath reached 80 °C, the zeolite-Y-encapsulated catalyst (0.025 g) was added to the reaction mixture which was continuously stirred. During the reaction, the products were periodically analysed using a gas chromatograph by withdrawing small aliquots, and their identities were confirmed by GC-MS. Various parameters, such as amounts of oxidant and catalyst as well as the temperature of the reaction mixture were studied in order to understand their effect on the conversion and patterns of the reaction products.

Oxidation of Cyclohexene: The catalytic oxidation of cyclohexene was also carried out using [Cu(pydx-en)]-Y and [Cu(pydx-1,3-pn)]-Y. Aqueous 30% H_2O_2 (2.28 g, 20 mmol), cyclohexene (0.82 g, 10 mmol) and catalyst (0.025 g) were mixed in acetonitrile (20 mL), and the reaction mixture was heated at 75 °C with continuous stirring in an oil bath. The progress of the reaction was monitored as mentioned above. The identification of the various products was confirmed by GC-MS.

Oxidation of Methyl Phenyl Sulfide: Aqueous 30% H_2O_2 (2.28 g, 20 mmol) and catalyst (0.025 g) were added to a solution of methyl phenyl sulfide (1.24 g, 10 mmol) dissolved in acetonitrile (20 mL), and the reaction mixture was stirred at ambient temperature for 3 h. The formation of the reaction products was monitored by GC.

Measurement of UV/Vis Spectra by Adding H_2O_2 : A solution of complex **1** or **2** in methanol (ca. 10^{-4} M, 10 mL) was prepared and

the UV spectra measured. A solution of H_2O_2 was prepared by dissolving five drops of 30% H_2O_2 in methanol (5 mL). One drop of this H_2O_2 solution was added and the UV spectra recorded again. Several similar additions were made, and after each addition the spectral changes were recorded similarly. As the solubility of complexes **1** or **2** is low in methanol, only the UV region could be covered in this way. For the visible region, the complexes were dissolved in DMSO (concentration about 10^{-3} M, 10 mL), and additions of the H_2O_2 solution were made similarly, now recording the visible region of the spectra (see insets of Figures 21 and 22).

Acknowledgments

The authors are thankful to the Council of Scientific and Industrial Research, New Delhi for financial assistance. The authors also wish to thank FEDER, Fundação para a Ciência e a Tecnologia and POCI 2010 (ref. POCI/QUI/55985/2004) for financial support, and Kamila Koci for the ESI-MS experiments.

- [1] J. Poltowicz, K. Pamin, E. Tabor, J. Haber, A. Adamski, Z. Sojka, *Appl. Catal. A* **2006**, *299*, 235–242.
- [2] S. P. Verkey, C. Ratnasamy, P. Ratnasamy, *J. Mol. Catal. A* **1998**, *135*, 295–306.
- [3] S. P. Verkey, C. Ratnasamy, P. Ratnasamy, *Microporous Mesoporous Mater.* **1998**, *22*, 465–474.
- [4] S. P. Verkey, C. Ratnasamy, P. Ratnasamy, *Appl. Catal. A* **1999**, *182*, 91–96.
- [5] S. Deshpande, D. Srinivas, P. Ratnasamy, *J. Catal.* **1999**, *188*, 261–269.
- [6] D. Chatterjee, A. Mitra, *J. Mol. Catal. A* **1999**, *144*, 363–367.
- [7] C. Bowers, P. K. Dutta, *J. Catal.* **1990**, *122*, 271–279.
- [8] M. S. Niassary, F. Farzaneh, M. Ghandi, L. Turkian, *J. Mol. Catal. A* **2000**, *157*, 183–188.
- [9] M. Silva, C. Freire, B. de Castro, J. L. Figueiredo, *J. Mol. Catal. A* **2006**, *258*, 327–333.
- [10] T. Joseph, S. B. Halligudi, C. Satyanarayan, D. P. Sawant, S. Gopinathan, *J. Mol. Catal. A* **2001**, *168*, 87–97.
- [11] M. R. Maurya, S. J. J. Titinchi, S. Chand, *Appl. Catal. A* **2002**, *228*, 177–187.
- [12] M. R. Maurya, S. J. J. Titinchi, S. Chand, *J. Mol. Catal. A* **2003**, *201*, 119–130.
- [13] M. R. Maurya, M. Kumar, S. J. J. Titinchi, H. S. Abbo, S. Chand, *Catal. Lett.* **2003**, *86*, 97–105.
- [14] M. R. Maurya, A. K. Chandrakar, S. Chand, *J. Mol. Catal. A: Chem.* **2007**, *270*, 225–235.
- [15] I. Correia, J. Costa Pessoa, M. T. Duarte, R. T. Henriques, M. F. M. Piedade, L. F. Veiros, T. Jackusch, A. Dornyei, T. Kiss, M. M. C. A. Castro, C. F. G. C. Geraldes, F. Avecilla, *Chem. Eur. J.* **2004**, *10*, 2301–2317.
- [16] I. Correia, A. Dornyei, T. Jakusch, F. Avecilla, T. Kiss, J. Costa Pessoa, *Eur. J. Inorg. Chem.* **2006**, 2819–2830.
- [17] I. Correia, A. Dornyei, T. Jakusch, F. Avecilla, T. Kiss, J. Costa Pessoa, *Eur. J. Inorg. Chem.* **2006**, 656–662.
- [18] M. Valko, *Inorg. Chem.* **1993**, *32*, 4131–4138.
- [19] H. Elias, *Angew. Chem. Int. Ed. Engl.* **1992**, *31*, 623–625.
- [20] D. F. Evans, *J. Chem. Soc.* **1959**, 2003–2005.
- [21] E. Sinn, A. B. Blake, W. Haussain, R. Paschke, J. R. Chipperfield, *Inorg. Chem.* **1995**, *34*, 1125–1129.
- [22] J. Peisach, W. E. Blumberg, *Arch. Biochem. Biophys.* **1974**, *165*, 691–708.
- [23] U. Sakaguchi, A. W. Addison, *J. Chem. Soc. Dalton Trans.* **1979**, 600–608.
- [24] V. T. Kasumov, F. Koksai, *Spectrochim. Acta Part A* **2005**, *61*, 225–231.
- [25] K. M. Ananth, M. Kanthimathi, B. U. Nair, *Transition Met. Chem.* **2001**, *26*, 333–338.
- [26] V. Hulea, E. Dumitriu, *Appl. Catal. A* **2004**, *277*, 99–106.

- [27] M. R. Maurya, U. Kumar, P. Manikandan, *Dalton Trans.* **2006**, 3561–3575.
- [28] M. R. Maurya, U. Kumar, P. Manikandan, *Eur. J. Inorg. Chem.* **2007**, 2303–2314.
- [29] A. Butler, M. J. Clague, G. E. Meister, *Chem. Rev.* **1994**, *94*, 625–638.
- [30] M. R. Maurya, A. K. Chandrakar, S. Chand, *J. Mol. Catal. A: Chem.* **2007**, *263*, 227–237.
- [31] E. I. Solomon, P. Chen, M. Metz, S.-K. Lee, A. E. Palner, *Angew. Chem. Int. Ed.* **2001**, *40*, 4570–4590.
- [32] J. P. Klinman, *Chem. Rev.* **1996**, *96*, 2541–2561.
- [33] K. D. Karlin, J. C. Hayes, Y. Gultneh, R. W. Cruse, J. W. McKown, J. P. Hutchinson, J. Zubieta, *J. Am. Chem. Soc.* **1984**, *106*, 2121–2128.
- [34] A. Rockenbauer, L. Korecz, *Appl. Magn. Reson.* **1996**, *10*, 29–43.
- [35] G. M. Sheldrick, *SHELXTL*, release 5.1, Bruker Analytical X-ray Systems, Madison, WI, **1997**.

Received: July 27, 2007

Published Online: November 8, 2007